

Short Communication

Effect of Heat Treatment on the Properties of Ultrasonic Pulse Electrodeposited Ni-W-P/Al₂O₃-LaCl₃ Composite Coatings

Qingwei Niu¹, Zili Li^{1,*}, Gan Cui¹, Guodong Liu², Bingying Wang²

¹ College of Pipeline and Civil Engineering, China University of Petroleum, Qingdao 266580, China

² College of Mechanical and Electrical Engineering, China University of Petroleum, Qingdao 266580, China

*E-mail: zilimenzhu@163.com

Received: 6 January 2017 / Accepted: 23 March 2017 / Published: 12 May 2017

Ni-W-P/Al₂O₃-LaCl₃ composite coatings were prepared by ultrasonic pulse electrodeposition using a N80 steel matrix. The structural features and other properties of the composite coatings were analyzed using metallographic measurements, micro-hardness measurements, scanning electron microscopy, X-ray diffraction, and electrochemical measurements. The effect of heat treatment on the composite coatings' microstructures and micro-hardnesses was also investigated. The micro-hardnesses of the composite coatings increased when the temperature of heat treatment was increased up to 400 °C. However, at higher heat-treatment temperatures, micro-hardness decreased, because new Ni₃P and Ni₄W phases were generated after heat treatment. At a heat-treatment temperature of 400 °C, the composite coating had the highest corrosion resistance.

Keywords: Heat treatment; Composite coating; Ultrasonic pulse electrodeposition; Corrosion resistance

1. INTRODUCTION

In recent years, composite coating materials have developed rapidly. Because of their excellent anti-friction, electrically insulating, and corrosion-resistance properties, composite coatings are widely used in a variety of fields, including chemical engineering, medical science, machine manufacturing, and the electronics industry [1-4]. To date, many methods have been reported to prepare composite coatings. Compared to chemical and spray deposition methods, electrodeposition is a more useful surface modification technique for the preparation of composite coatings, because it is more controllable and results in a more strongly adhered coating [5,6]. Among the reported electrodeposition methods, pulse electrodeposition is more widely used than direct electrodeposition, because pulse

electrodeposition can form composite coatings with smaller grains, superior hardnesses and wear resistances, and higher corrosion resistances [7-10]. However, some studies have shown that Ni-P, Ni-W, and Ni-W-P coatings have poor performances. Therefore, new approaches are needed to use rare earth elements or nanoparticles in composite coatings.

According to several recent studies, rare earth elements and nanoparticles provide increased hardness, improved wear properties, and a higher corrosion resistance [11-13]. Wasekar et al. [12] reported that the addition of SiC to Ni-W composite coatings enhanced their hardness and modulus at a SiC loading of up to 5vol.%. Beltowska-Lehman et al. [13] found that the hardness and wear behavior of a Ni-W composite coating improved after the addition of Al₂O₃ particles. The Al₂O₃ content and distribution was essential for this improved performance. Moreover, the microstructures and microhardnesses of the composite coatings changed when the amount of rare earth element in the coatings was varied. However, few studies have focused on simultaneously adding rare earth elements and nanoparticles to a composite coating at the same time.

In this work, a rare earth element and alumina nanoparticles were added simultaneously to a Ni-W-P composite coating, which was prepared in a mixed bath. The effect of heat treatment was then investigated on the hardness and corrosion resistance of the composite coatings.

2. EXPERIMENTAL

2.1. Experimental materials

Ni-W-P/Al₂O₃-LaCl₃ composite coatings containing a rare earth element and Al₂O₃ nanoparticles were prepared by pulse current electrodeposition in a citrate solution. The compositions of the mixed bath containing Na₃Cit, NiSO₄, and Na₂WO₄ are shown in Table 1. LaCl₃ (the source of rare earth element) and Al₂O₃ nanoparticles were also added at concentrations of 1 g/L and 20 g/L, respectively. The mixed bath was maintained at pH 9 through the regular addition of sulfuric acid (H₂SO₄) and ammonia (NH₃·H₂O). The mixed bath was agitated using an ultrasonicator at 100 kHz and 300 W for 30 min before each experiment. The bath was prepared in distilled water using analytical grade reagents.

Table 1. Composition of the plating bath

Component	NiSiO ₄ ·6H ₂ O g/L	Na ₂ WO ₄ ·2H ₂ O g/L	Na ₂ H ₂ PO ₂ ·H ₂ O g/L	Na ₃ Cit g/L
Concentration	50	60	40	100

N80 steel plates with dimensions of 50 mm × 20 mm × 2 mm were used as cathodes. These plates were mechanically polished and cleaned before each experiment. To degrease and activate the cathodes' surfaces, the plates were immersed in hot 40 g/L NaOH containing 10% H₂SO₄ for ~10 min. The anode was a pure nickel plate. The anode-to-cathode surface area ratio was 3:1. In all experiments,

an ultrasonicator was used at 100 kHz and 300W, and the current density was maintained at 40 mA/cm² with a duty cycle of 0.4. The bath temperature was 60 °C. Electrodeposition proceeded for 1 h.

2.2. Experimental methods

Heat treatment was performed in a vacuum oven, in which the temperature increased from 200 °C to 600 °C at a rate of 10 °C/min. Samples were then cooled to room temperature. The samples' micro-hardnesses were measured with a micro-hardness tester under a load of 200 g for 15 s. The coatings' surface morphologies were observed using scanning electron microscopy (SEM), and their structures were analyzed with X-ray diffractometry at scanning angles of 10° to 90° at 4°/min.

A CHI660B electrochemical workstation was used to test corrosion resistance. A sample with a composite coating acted as the working electrode, while Pt and a saturated calomel electrode were used as the auxiliary and reference electrodes, respectively. The corrosion medium contained 3.5% NaCl, and experiments were performed at room temperature. Measurements were performed at a scan rate of 0.166 mV/s over the potential range from -150 mV to +300 mV from the open circuit potential.

3. RESULTS AND DISCUSSION

3.1 Morphology and microstructure

XRD patterns of the as-plated and heat-treated Ni-W-P/Al₂O₃-LaCl₃ coatings are shown in Fig.1. Fig.1 (a, b) shows the XRD patterns of the as-plated coating and the coating that was heat treated at 200 °C. In the vicinity of $2\theta = 45^\circ$, there was a broad diffuse scattering peak, which indicated that the coating was an amorphous alloy [14]. Atoms could not diffuse a long distance at a temperature of only 200 °C. Instead, only small changes in position occurred along with structural relaxation, leaving the amorphous characteristics unchanged. The heat-treated coating remained non-crystalline without any newly formed phases. Amorphous materials have long-range disordered structure and short-range orderly structure. When the heat-treatment temperature was increased, phosphorus atoms in the alloy continuously diffused and aggregated, and the size of the semi-short-range ordered Ni-rich microstructures in the amorphous state gradually increased. The material then became crystalline when a critical nucleation size was reached. At higher heat-treatment temperatures, the XRD patterns of the Ni-W-P/Al₂O₃-LaCl₃ coatings changed. The coating shifted from an amorphous to a crystalline state when the heat-treatment temperature was increased to 400 °C. The Ni peak became narrower, and the alloy's degree of crystallization was greatly enhanced [14]. The coating's structure also changed significantly, new Ni₃P and Ni₄W phases were observed. These metastable phases were believed to be Ni_xP_y [15, 16]. Peaks for Al₂O₃ were not observed in the XRD patterns, probably due to the low quantity of Al₂O₃ particles and also the high intensity of Ni diffraction peaks [17].

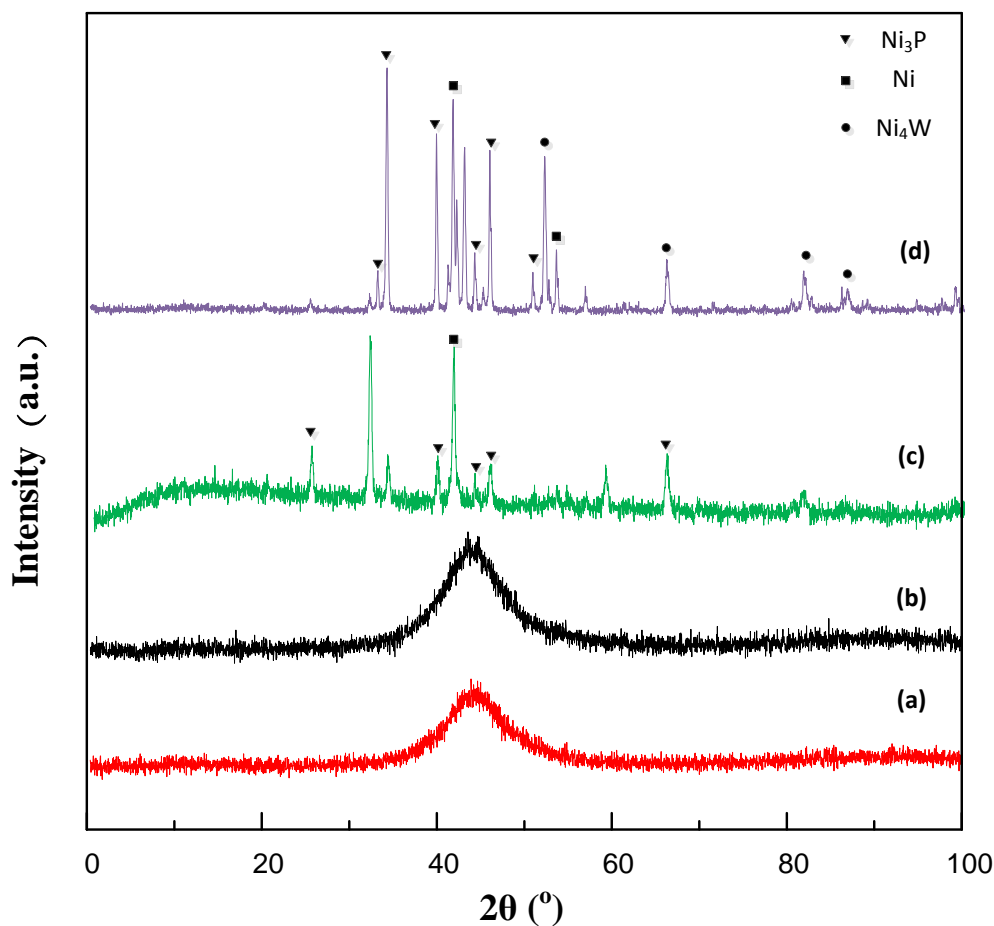
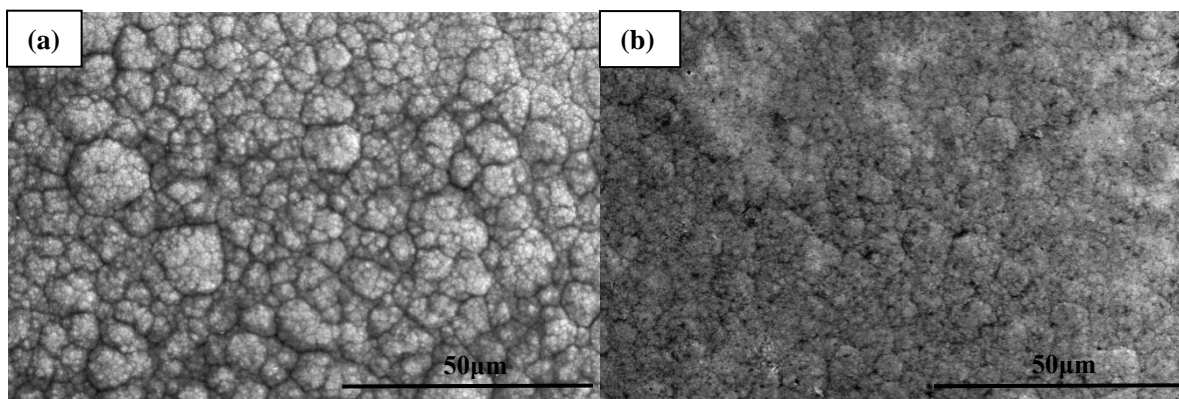


Figure 1. XRD patterns of Ni-W-P/ Al_2O_3 - LaCl_3 deposits (a) as-plated and after heat treatment at (b) 200 °C, (c) 400 °C and (d) 600 °C

Surface morphologies of the Ni-W-P/ Al_2O_3 - LaCl_3 composite coatings at different heat-treatment temperatures are shown in Fig.2. Below 200 °C, the surface changed only slightly compared to that of the as-plated coating. Only the degree of stromae on the surface decreased after heat treatment at 200 °C.



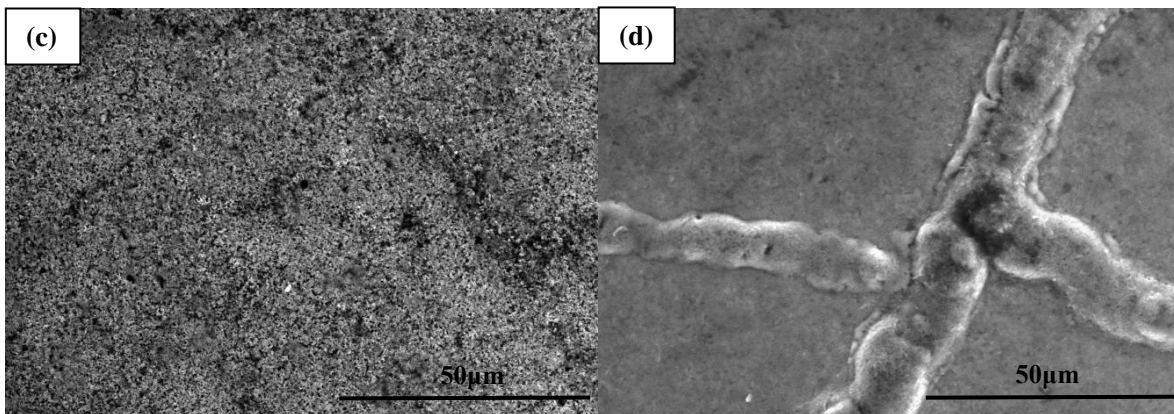


Figure 2. Surface morphologies of Ni-W-P/Al₂O₃-LaCl₃ composites (a) as-deposited and after heat treatment at (b) 200 °C, (c) 400 °C and (d) 600 °C

At a heat-treatment temperature of 400 °C, the composites’ surface morphologies became more continuous and compact with correspondingly smaller grains, because new Ni and P phases formed. Meanwhile, La and the Al₂O₃ nanoparticles became more evenly disperse in the matrix metal. When the heat-treatment temperature was increased to 600 °C, the surface of the composite coating remained compact and sequential. However, the grains became larger, likely because the aggregated nanoparticles hindered the formation of crystal nuclei, which are required for crystal growth [18].

3.2 Coating micro-hardness

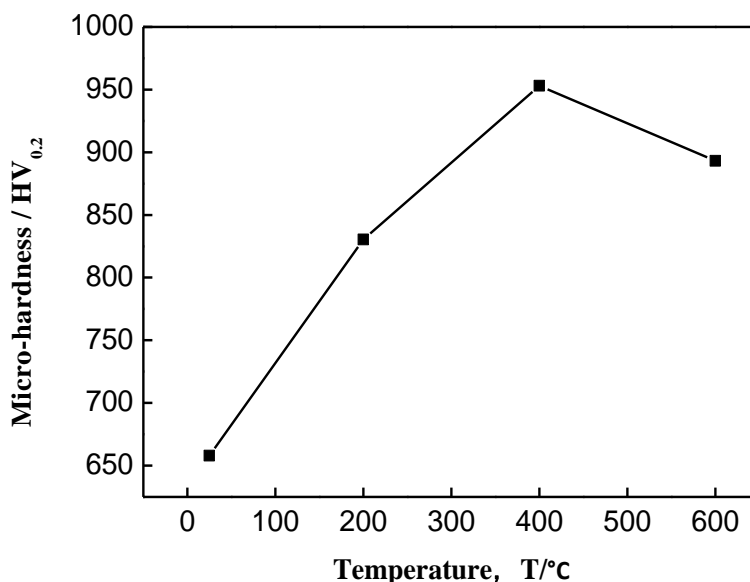


Figure 3. Effect of heat-treatment temperature on the coating’s micro-hardness

Fig.3 shows the effect of heat-treatment temperature on the micro-hardness of the electrodeposited Ni-W-P/Al₂O₃-LaCl₃ composite coating. As shown in Fig.3, micro-hardness initially increased with increasing heat-treatment temperature. At 400 °C, the micro-hardness reached its

maximum value of 951.2 HV_{0.2}, which was 295.2 HV_{0.2} higher than that of an as-deposited Ni-W alloy. Micro-hardness then decreased at higher heat-treatment temperatures, because the diffusion and migration of atoms on the matrix's surface was accelerated at higher temperatures, causing the formation of lattice distortions and the termination of dislocation motion. At a certain threshold temperature, additional Ni₃P and Ni₄W phases began to uniformly precipitate on the coating's surface, increasing its micro-hardness. However, above 400 °C, the Ni₃P phases combined, causing the grains to become coarser and softer [19] and lattice distortions to disappear. Therefore, the micro-hardnesses of these coatings decreased.

3.3 Corrosion tests

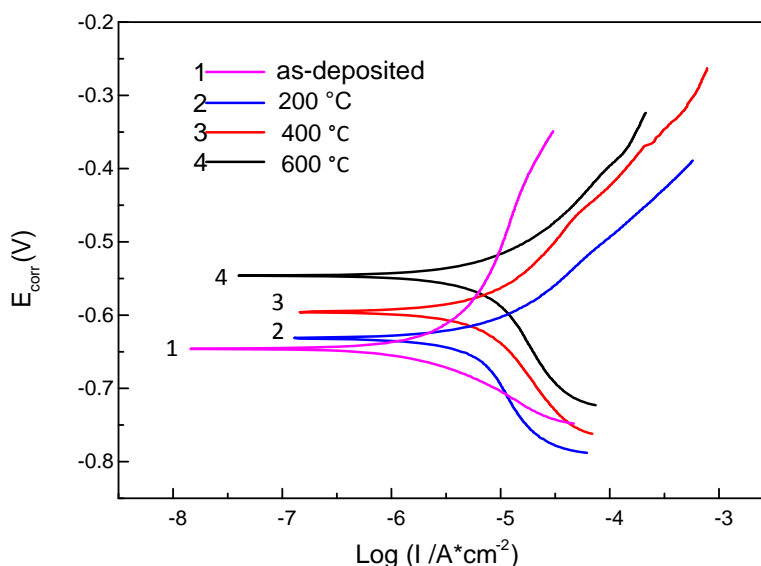


Figure 4. Potentiodynamic polarization curves of as-plated and heat-treated Ni-W-P/Al₂O₃-LaCl₃ nanocomposite coatings in 3.5 wt% NaCl

Table 2. Corrosion characteristics of Ni-W-P/Al₂O₃-LaCl₃ coatings in 3.5 wt% NaCl

Coating	As-plated	Heat treatment at 200 °C	Heat treatment at 400 °C	Heat treatment at 600 °C
<i>b_a</i> (mV)	113.59	96.998	135.91	102.95
<i>b_c</i> (mV)	-58.598	-270.38	-187.37	-182.79
<i>E_{corr}</i> (V)	-0.642	-0.625	-0.596	-0.547
<i>i_{corr}</i> (A/cm ²)	10.23	9.736	8.351	8.954

Polarization curves of Ni-W-P/Al₂O₃-LaCl₃ composite coatings with and without heat treatment are shown in Fig.4. Corrosion parameters were fit to these curves (Table 2). At a heat-treatment temperature of 400 °C, the self-corrosion potential reached its most positive value, and the corrosion current density was minimized. Therefore, this coating was the most corrosion resistant. The

Tafel slope obtained its maximum value at 400 °C, indicating that the reaction power decreased to its lowest value. This Tafel slope might have resulted from the newly formed phases on the compact surface. The denser and more homogenous composite structure prevented the movement of chloride ions into the coatings, leading to a lower corrosion rate [20].

4. CONCLUSIONS

(1) XRD results indicated that the as-plated coating had a similar composition and structure to that of a coating that was heat treated at 200 °C. The coating remained in the non-crystalline state, and no new phases formed.

(2) The coating's micro-hardness increased with increasing heat-treatment temperature and reached a maximum of 951.2 HV_{0.2} at 400 °C. This high micro-hardness resulted from the formation of new Ni₃P and Ni₄W phases.

(3) When the heat-treatment temperature was increased to 400 °C or higher, the surface morphologies of the composite coatings became more continuous and compact.

(4) Polarization curves of the as-plated and heat-treated composites indicated that heat treatment increased the corrosion resistance of Ni-W-P/Al₂O₃-LaCl₃. At a heat-treatment temperature of 400 °C, the coating had its highest corrosion resistance, possibly because new phases formed on the compact surface, preventing the movement of chloride ions into the coatings and slowing down the rate of corrosion.

ACKNOWLEDGEMENTS

The authors would like to acknowledge Mr. Zhan and Ms. Zhou for their technical assistance.

References

1. N. Elkhoshkhany, A. Hafnway and A. Khaled, *J. Alloys Compd.*, 695 (2017) 1505.
2. H. E. Mohammadloo and A. A. Sarabi, *Appl. Surf. Sci.*, 387 (2016) 252.
3. S. M. Liu, B. E. Li, C. Y. Liang, H. S. Wang and Z. X. Qiao, *Appl. Surf. Sci.*, 362 (2016) 109.
4. S. J. Algodí, J. W. Murray, M. W. Fay, A. T. Clare and P. D. Brown, *Surf. Coat. Technol.*, 307 (2016) 639.
5. Y. Zhou, F. Q. Xie, X. Q. Wu, W. D. Zhao and X. Chen, *J. Alloys Compd.*, 699 (2017) 366.
6. D. Almasi, S. Izman, M. Assadian, M. Ghanbari and M. R. A. Kadir, *Appl. Surf. Sci.*, 314 (2014) 1034.
7. A. Sharma, S. Bhattacharya, S. Das and K. Das, *Surf. Eng.*, 65 (2015) 378.
8. A. Sharma, S. Bhattacharya, S. Das and K. Das, *Metall. Mater. Trans. A*, 45 (2014) 4610.
9. K. A. Kumar, G. P. Kalaignan and V. S. Muralidharan, *Ceram. Int.*, 39 (2013) 2827.
10. M. Guo, X. R. Zhu and H. J. Li, *J. Alloys Compd.*, 657 (2016) 336.
11. E. Beltowska-Lehman, P. Indyka, A. Bigos, M. J. Szczerba and M. Kot, *J. Electroanal. Chem.*, 775 (2016) 27.
12. N. P. Wasekar, S. M. Latha, M. Ramakrishna, D. S. Rao and G. Sundararajan, *Mater. Des.*, 112 (2016) 140.
13. E. Beltowska-Lehman, P. Indyka, A. Bigos, M. Kot and L. Tarkowski, *Surf. Coat. Technol.*, 211 (2012) 62.
14. Y. Wang, Q. Zhou, K. Li, Q. Zhong and Q. B. Bui, *Ceram. Int.*, 41 (2015) 79.

15. C. Ma, F. Wu, Y. Ning, F. Xia and Y. Liu, *Ceram. Int.*, 40 (2014) 9279.
16. H. Liu, R. Guo and Z. Liu, *T. Nonferr. Metal. Soc.*, 22 (2012) 3012.
17. Z. Shafiee, M. E. Bahrololoom and B. Hashemi, *Mater. Des.*, 108 (2016) 19.
18. Y. C. Wang, D. P. Zhao, S. K. Li, J. X. Liu and F. C. Wang, *Mater. Sci. Eng. A*, 547 (2012) 104.
19. S. Duari, A. Mukhopadhyay, T. K. Barman and P. Sahoo, *Surf. Interface Anal.*, 6 (2017) 177.
20. S. Dehgahi, R. Amini and M. Alizadeh, *J. Alloys Compd.*, 692 (2017) 622.

© 2017 The Authors. Published by ESG (www.electrochemsci.org). This article is an open access article distributed under the terms and conditions of the Creative Commons Attribution license (<http://creativecommons.org/licenses/by/4.0/>).